Available online at www.sciencedirect.com
ScienceDirect
Trans. Nonferrous Met. Soc. China 33(2023) 755−764
Transactions of Nonferrous Metals Society of China
www.tnmsc.cn

DFT study on termination stabilities of $Mg_{17}Al_{12}$ (110) surface

Jia-jia WANG[1], Zi-jie LU[1], Kai-xiao ZHANG[2], Guo-bing YING[1],
Bao-song LI[1], Jian-qing CHEN[1], Dan SONG[1], Jing-hua JIANG[1], Ai-bin MA[1]

1. College of Mechanics and Materials, Hohai University, Nanjing 210098, China;
2. College of Science, Hohai University, Nanjing 210098, China

Received 17 November 2021; accepted 25 February 2022

Abstract: The $Mg_{17}Al_{12}$ (110) surface has five possible terminations (T1−T5). The T3 termination has been regarded as the most stable termination for long time, whereas recent theoretical calculations have revealed that the T1 termination is the most stable one. To solve the dispute, density functional theory calculations were performed in this study to unravel the most stable termination of $Mg_{17}Al_{12}$ (110) surface. Surface energy calculation results show that, whether defects are considered or not, the T1 termination is always the most stable termination of $Mg_{17}Al_{12}$ (110) surface. The stability of T1 termination may be ascribed to the Al truncated-tetrahedron because only cutting $Mg_{17}Al_{12}$ along T1 termination of (110) surface will not destroy the integrity of Al truncated-tetrahedron. In addition to unraveling the most stable termination, work functions of $Mg_{17}Al_{12}$ (110) surface were also calculated. The results show that the work function of $Mg_{17}Al_{12}$ (110) surface is mainly controlled by concentration of surface Al_{Mg} defects.
Key words: $Mg_{17}Al_{12}$; surface termination; density functional theory; surface energy; work function

1 Introduction

The $Mg_{17}Al_{12}$ phase, which is a dominant intermetallic compound in Mg−Al alloys, plays a critical role in the mechanical and corrosion performances of Mg−Al alloys [1,2]. The $Mg_{17}Al_{12}$ phase is also a potential hydrogen storage material with 4.4 wt.% maximum hydrogen storage capacity [3]. No matter as an intermetallic compound or as a hydrogen storage material, surface property of $Mg_{17}Al_{12}$ is a key factor that affects its performances. Therefore, it is necessary to investigate and understand surface properties of $Mg_{17}Al_{12}$.

Theoretical calculations such as molecular dynamics (MD) and density functional theory (DFT) are effective methods to investigate surface properties from the atomic level. To the best of our knowledge, the $Mg_{17}Al_{12}$ (110) surface has been extensively studied by theoretical calculations because the (110) surface is more stable than other surfaces such as (100) and (111) surfaces [4,5]. Furthermore, in Mg−Al alloys, the β-$Mg_{17}Al_{12}$ precipitates have a $(110)_\beta//(0001)_\alpha$ Burgers orientation relationship with α-Mg matrix [6], suggesting that the (110) surface is crucial for the applications of $Mg_{17}Al_{12}$.

In surface calculations, a reasonable surface model is the essential prerequisite to obtain reliable results. When a surface contains more than one termination, choosing a suitable termination to bulid a surface model is particularly important. As can be seen in Fig. 1, the $Mg_{17}Al_{12}$ (110) surface contains five possible terminations, which are labeled as T1−T5, respectively. To the best of our knowledge, some theoretical researchers chose T3 termination as the top surface to build $Mg_{17}Al_{12}$

Corresponding author: Guo-bing YING, Tel: +86-25-83787239, Fax: +86-25-83786046, E-mail: yinggb2010@126.com;
Bao-song LI, Tel: +86-25-83787239, E-mail: lbs79@126.com
DOI: 10.1016/S1003-6326(23)66143-6
1003-6326/© 2022 The Nonferrous Metals Society of China. Published by Elsevier Ltd & Science Press

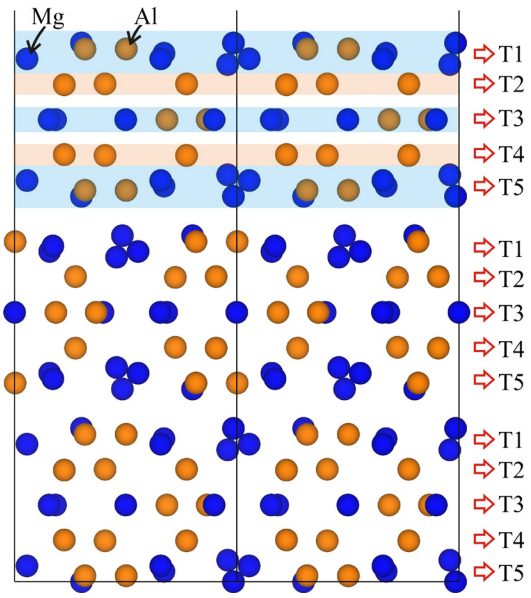

Fig. 1 Atomic structure of $Mg_{17}Al_{12}$ (110) surface (The first T1−T5 terminations are indicated by shading)

(110) surface model [7−10]. This may be ascribed to two advantages of this termination. Firstly, all atoms on T3 termination are in the same plane (with the same *z*-axis coordinate values), which is very helpful to manually build surface model. Secondly, unlike the T2 and T4 terminations which only include Al atoms, the T3 termination consists of both Al and Mg atoms. This is convenient for T3 termination to be used to investigate different surface intrinsic defects or H_2 adsorption on different surface atomic sites. Among the T1−T5 terminations, only the T3 termination has these two advantages.

However, the two advantages of the T3 termination do not guarantee that this termination is thermodynamically stable as the top $Mg_{17}Al_{12}$ (110) surface. Therefore, it is necessary to compare surface energies of T1−T5 terminations. So far, only WANG and LI [5] have calculated surface energies of $Mg_{17}Al_{12}$ (110) surface with different terminations and revealed that T1 termination was more stable than other terminations. However, some improvements are still needed based on Ref. [5]. Firstly, only the most stable (T1) and unstable (T2) terminations were discussed in their work, while surface energies of other terminaitons (T3−T5) were not provided. Secondly, they only considered pure terminations and neglected defect doping effects. When intrinsic defects, for example the Mg vacancies, are doped, surface energies of T1−T5 terminations may change. Therefore, defect doping effects should be considered to prove that T1 is really the most stable termination. Besides theoretical work, recent experiment also indicated that the $Mg_{17}Al_{12}$ (110) surface interacted with Mg (0001) matrix through T1 termination rather than T3 termination [11], further suggesting that T3 termination may be not as stable as expected.

The above discussion reveals that the most stable termination of $Mg_{17}Al_{12}$ (110) surface remains controversial. Since the (110) surface is very crucial for practical applications of $Mg_{17}Al_{12}$, it is necessary to investigate and resolve termination problems of $Mg_{17}Al_{12}$ (110) surface. In this study, based on DFT calculations, the $Mg_{17}Al_{12}$ (110) surface with all possible terminations will be systematically investigated. In addition to unraveling stable terminations, work function of $Mg_{17}Al_{12}$ (110) surface with intrinsic defects will be calculated. This study is expected to provide useful guidance for future investigations of $Mg_{17}Al_{12}$, especially where surface and interface reactions are involved.

2 Computational methods

2.1 Computational details and models

All DFT calculations are performed using VASP [12] (Version 5.2) coded with a projected augmented wave (PAW [13]) method. The generalized gradient approximation (GGA [14]) in the scheme of Perdew–Burke–Ernzerhof (PBE [15]) is selected as the exchange correlation function. The cutoff energy is 400 eV. Geometry relaxations are performed until the residual forces on each ion converge to be smaller than 0.02 eV/Å. For Mg and Al elements, the $3s^2$ and $3s^23p^1$ orbits, respectively, are treated as valence states. Based on these computational parameters, the conventional cell of $Mg_{17}Al_{12}$ is firstly relaxed. The relaxed lattice constants of cubic $Mg_{17}Al_{12}$ are $a=b=c=10.52$ Å, which are consistent with the estimated experimental uncertainty (10.54 Å [16]). Then, the $Mg_{17}Al_{12}$ (110) surface can be constructed from the relaxed bulk $Mg_{17}Al_{12}$.

Figure 2(a) shows the slab model of $Mg_{17}Al_{12}$ (110) surface used in this study. As mentioned above, the $Mg_{17}Al_{12}$ (110) surface consists of five possible terminations. The T2−T4 terminations are obvious to identify because the atoms of each

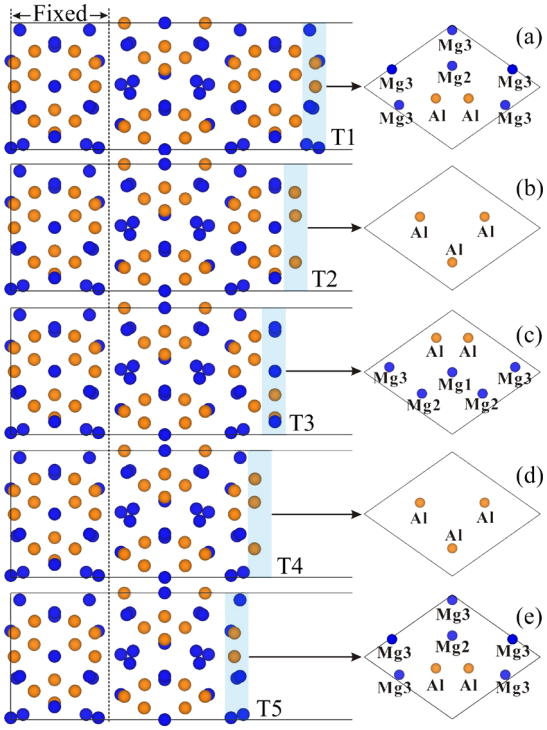

Fig. 2 Slab models of $Mg_{17}Al_{12}$ (110) surface with T1−T5 (a−e) terminations (The atomic arrangement of top layer is also shown)

termination are in the same plane. In contrast, atoms of T1 and T5 terminations are in disorder. It is very difficult to find out atoms which are in the same plane from T1 and T5 terminations. Therefore, all atoms of T1 (the same as T5) termination are simply treated as a single atomic layer, agreeing with the termination classification method in Ref. [5]. As can be seen in Fig. 2(a), the T1−T5 terminaions consistute one repeated unit. Convergence test reveals that three repeated units are siffucient to simulate the $Mg_{17}Al_{12}$ (110) surface (see SI-1 of Supporting Information for more details of convergence test). During geometry relaxations, the bottom five atomic layers are fixed. Due to the asymmetric model, dipole correction has been added in all calculations.

In this study, since effects of intrinsic defects on surface stability will be considered, it is necessary to discuss atomic composition of different terminations, especially the T1 and T3 terminations. Figures 2(a) and (c) show top view of T1 and T3 terminations, respectively. Note that, although the atomic composition of T5 termination is the same as that of T1 termination, they are different terminations because they have different sublayers (the same as T2 and T4). The atomic positions of $Mg_{17}Al_{12}$ can be grouped into four different sublattices [17]: three inequivalent lattice sites for Mg (with Wyckoff position 2a, 8c and 24g, which are named Mg1, Mg2 and Mg3, respectively, in this study), and the 24 g lattice site for Al. The T1 termination contains 2Al, 1Mg2 and 5Mg3 atoms. The T3 termination contains all four sublattices (2Al, 1Mg1, 2Mg2 and 2Mg3).

2.2 Surface energy calculation method

Surface energy (E_s) is calculated by the following equation [18]:

$$E_s = (E_{slab} - \sum_i n_i\mu_i)/A - S_{bottom} \quad (1)$$

where E_{slab} is the total energy of slab model, n_i and μ_i (i=Mg and Al) are the number and chemical potential of constituent i, respectively, A is the surface area of slab model, and S_{bottom} is the surface energy of the fixed bottom surface. Since the bottom five atomic layers are fixed during calculations, the energy term S_{bottom} must be subtracted to obtain correct surface energy. The S_{bottom} is surface energy calculated by using a slab model which has identical terminations on both sides of the slab without geometry relaxation. More discussion of the S_{bottom} term can be found in SI-1 in the Supporting Information and our previous theoretical work [18].

As can be seen in Eq. (1), surface energies are dependent on the chemical potentials. Under thermal equilibrium growth conditions, $Mg_{17}Al_{12}$ should satisfy

$$17\Delta\mu_{Mg}+12\Delta\mu_{Al}=E^f \quad (2)$$

where $\Delta\mu_{Mg}$ (the same as $\Delta\mu_{Al}$) is energy difference between the chemical potential of Mg (μ_{Mg}) and energy per atom of bulk Mg (E_{Mg}), and E^f is formation energy of bulk $Mg_{17}Al_{12}$. The calculated E^f of $Mg_{17}Al_{12}$ (−0.753 eV) in this study agrees with other theoretical value (−0.609 eV [19]). Then, $\Delta\mu_{Al}$ and $\Delta\mu_{Mg}$ under different growth conditions can be obtained: under Al-rich (i.e., Mg-poor) growth condition, $\Delta\mu_{Al}$=0 eV and $\Delta\mu_{Mg}=E^f/17$=−0.044 eV; under Al-poor (i.e., Mg-rich) growth condition, $\Delta\mu_{Al}=E^f/12$=−0.063 eV and $\Delta\mu_{Mg}$=0 eV.

3 Results and discussion

3.1 Surface energies

Figure 3 shows surface energies of $Mg_{17}Al_{12}$

(110) surface with undoped T1−T5 terminations as a function of Al chemical potential. It is clearly seen that, in the whole range of Al chemical potentials, surface energy of T1 termination is much lower than that of other terminations. The T3 termination, which was expected to be the most stable termination in previous work [7−10], is only more stable than T2, T4 and T5 terminations. Our calculation result suggests that T1 and T2 terminations are theoretically the most stable and unstable terminations of $Mg_{17}Al_{12}$ (110) surface, respectively, agreeing with results obtained from MD method [5]. Figure 3 also reveals that, with the variation of Al chemical potential, surface enengies of all five terminations do not vary a lot. The surface energy variation line of T1 termination is even close to horizontal line. This means that the stability of $Mg_{17}Al_{12}$ (110) surface is nearly independent of growth conditions.

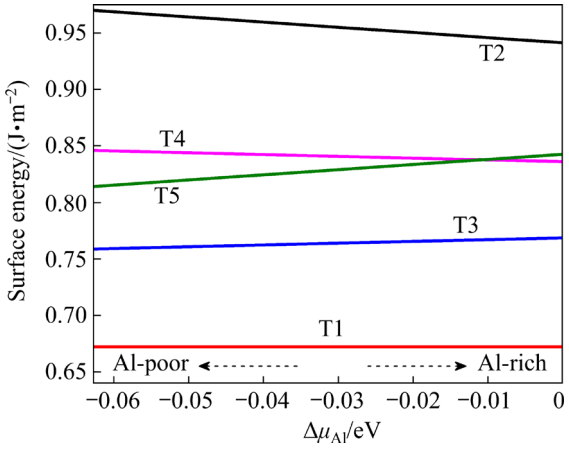

Fig. 3 Surface energies of $Mg_{17}Al_{12}$ (110) surface with non-defective T1−T5 terminations as function of Al chemical potential $\Delta\mu_{Al}$

To make a detailed comparison with other theoretical work, surface energies in Fig. 3 are further listed in Table 1. Note that, other theoretical work did not consider chemical potentials thus only one surface energy data was given. It is seen that both DFT and MD methods are used by XIAO et al [4] to calculate surface energy of T1 termination. Their DFT result (0.66 J/m^2) is in good agreement with our DFT result (0.67 J/m^2). A few years later, based on MD method again, WANG and LI [5] obtained the totally same surface energy of T1 termination (0.72 J/m^2), proving the MD result of XIAO et al [4]. Although the MD results of WANG and LI [5] are larger than our DFT results, the relative error of surface energies between T1 and T2 terminations calculated by MD are nearly the same as that by DFT. Moreover, their MD results also concluded that T1 and T2 were the most stable and unstable terminations, respectively. Therefore, the above discussion reveals that MD results are as reliable as DFT results, at least in the investigation of $Mg_{17}Al_{12}$ (110) surface. The reliability of MD method, as well as its high efficiency compared with DFT method, suggests that MD method may be more suitable to investigate large scale system. This is probably why the MD method is also used to calculate $Mg_{17}Al_{12}$/Mg interfaces in Ref. [5]. The surface energy of T3 termination calculated by ZHANG et al (0.66 J/m^2) [7] is lower than that in this study (0.76 J/m^2), which may be ascribed to different numbers of atomic layers in their (5 layers) and our (13 layers) work.

Table 1 Surface energies of $Mg_{17}Al_{12}$ (110) surface with different terminations (This study provides surface energies under Al-poor and Al-rich limit growth conditions; Data calculated by molecular dynamics method are marked with "MD")

Source	Termination	Surface energy/(J·m^{-2})	
		Al-poor	Al-rich
This study	T1	0.67	0.67
	T2	0.97	0.94
	T3	0.76	0.77
	T4	0.85	0.84
	T5	0.81	0.84
XIAO et al [4]	T1	0.66, 0.72 (MD)	
WANG and LI [5]	T1	0.72 (MD)	
	T2	1.01 (MD)	
ZHANG et al [7]	T3	0.66	

Although it can be seen from Fig. 3 that T1 termination is the most stable termination of $Mg_{17}Al_{12}$ (110) surface, the correctness of this conclusion is still doubtful because surface defects are not considered in Fig. 3. It is well known that practical materials usually contain various defects, which may affect surface stabilities. The $Mg_{17}Al_{12}$ phase in practice exhibits Al-rich off-stoichiometric compositions [20−22]. Theoretical work also revealed that Mg vacancy (V_{Mg}) and Al-substituted Mg anti-site (Al_{Mg}) intrinsic defects were more easily formed in $Mg_{17}Al_{12}$ [22], agreeing with the

Al-rich composition of $Mg_{17}Al_{12}$. When V_{Mg} or Al_{Mg} defects are doped into $Mg_{17}Al_{12}$ (110) surface, the stability order of T1 and T3 terminations may change. Therefore, to unravel true stable termination of $Mg_{17}Al_{12}$ (110) surface, it is necessary to further investigate effects of V_{Mg} or Al_{Mg} defects doped on T1 and T3 terminations.

Figures 4 and 5 show surface energies of T1 and T3 terminaitons, respectivley, doped with various defects as a function of Al chemical potential. Putting all data into one figure is not convenient to read. Then, surface energies of T1 termination doped with V_{Mg} and Al_{Mg} are shown in Figs. 4(a) and (b), respectively. Surface energies of T3 termination doped with V_{Mg} and Al_{Mg} are shown in Figs. 5(a) and (b), respectively. As mentioned in Fig. 2, the T1 and T3 terminations contain (1Mg2, 5Mg3) and (1Mg1, 2Mg2, 2Mg3) atoms, respectively. To investigate effects of defect concentration change on surface stability, different numbers of V_{Mg} or Al_{Mg} defects will be doped. For example, T1 termination doped with three V_{Mg3} is denoted as T1+3V_{Mg3}.

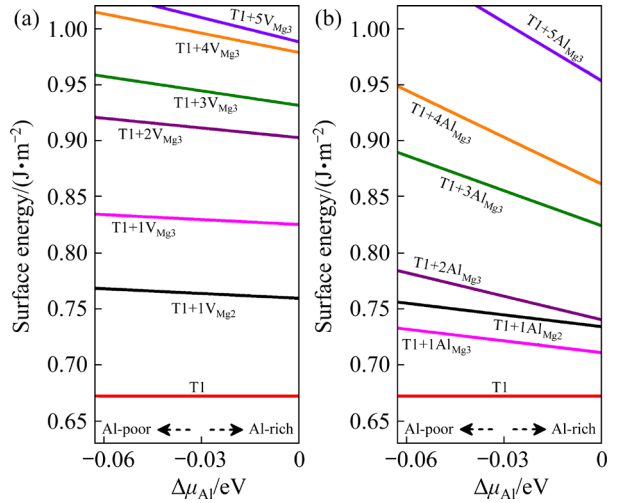

Fig. 4 Surface energies of T1 terminaiton with V_{Mg} (a) and Al_{Mg} (b) defects as function of Al chemical potential $\Delta\mu_{Al}$

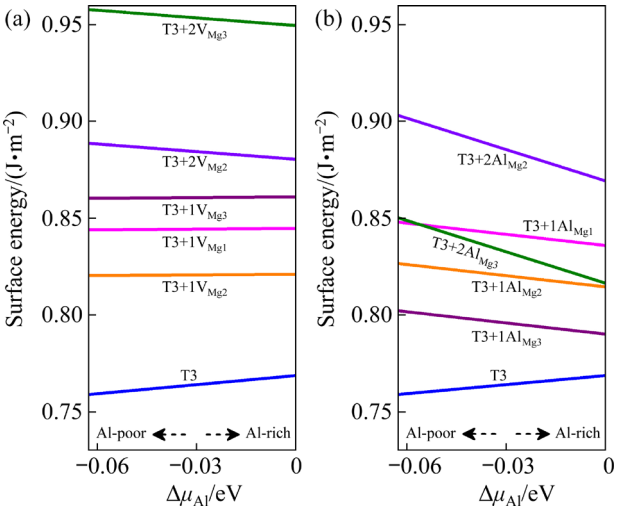

Fig. 5 Surface energies of T3 termination with V_{Mg} (a) and Al_{Mg} (b) defects as function of Al chemical potential $\Delta\mu_{Al}$

Figures 4 and 5 reveal that: (1) regardless of defect type, surface energies of undoped T1 and T3 terminations are lower than those of defective T1 and T3 terminations, respectively. Furthermore, with the increase of defect concentration, surface energies of defective T1 and T3 terminations gradually increase. This means that both the V_{Mg} and Al_{Mg} defects, especially in high concentrations, are not beneficial to the stability of $Mg_{17}Al_{12}$ (110) surface. The defect combinations are not considered because there are too many possible combinations. We tried to build some defect combinations and found that surface energies of defect combinations doped terminations were much higher. WANG et al [21] also found that defect combinations made the crystal structure of bulk $Mg_{17}Al_{12}$ metastable. (2) In given Mg lattice sites, terminations with Al_{Mg} anti-site defects are stabler than those with V_{Mg} defects, especially under the Al-rich growth condition. For example, in two given Mg3 lattice sites, surface energy of T1+2Al_{Mg3} is lower than that of T1+2V_{Mg3}. This means that Al_{Mg} anti-site defects are energetically more favorable than Mg vacancies on the $Mg_{17}Al_{12}$ (110) surface. SHIN and WOLVERTON [22] calculated defect formation energies of bulk $Mg_{17}Al_{12}$ and concluded that anti-site defects energetically favored over vacancy defects, agreeing with surface energy results in this study. (3) Vacancies at Mg2 lattice sites bring about lower surface energies. In contrast, anti-site defects at Mg3 lattice sites bring about lower surface energies. This means that Mg vacancy and Al_{Mg} anti-site defects energetically prefer Mg2 and Mg3 lattice sites of $Mg_{17}Al_{12}$ (110) surface, respectively, which is also in agreement with previous defect formation energy results [22].

The above discussion reveals that, although the defect doping effects are considered, T1 termination is still more stable than T3 termination. Therefore, surface energy results of Figs. 3−5 strongly prove that T1 termination is indeed the most stable termination of $Mg_{17}Al_{12}$ (110) surface.

3.2 Termination stabilities

To understand why T1 termination is the most stable termination, it is firstly necessary to understand bulk properties of $Mg_{17}Al_{12}$. Figure 6(a) shows atomic structure of $Mg_{17}Al_{12}$ conventional cell. When all Al atoms in the cell are connected with bonds, twelve Al atoms form an Al truncated-tetrahedron (four Al-triangles in the cell corner belong to Al truncated-tetrahedron of the adjacent period cells). This Al truncated-tetrahedron is composed of four equilateral triangular and four equilateral hexagonal faces (Fig. 6(b)). The chemical bonding of $Mg_{17}Al_{12}$ presents mixed bonding characteristic. The Al−Al pair in $Mg_{17}Al_{12}$ shows metallic and covalent characteristics (Fig. 6(c)), respectively. Then, due to the strong covalent characteristic of Al−Al pair and the geometric structure of Al truncated-tetrahedron, the bonding of Al truncated-tetrahedron is expected to be too strong to break. When the $Mg_{17}Al_{12}$ cell is extended to super-cell (Fig. 6(d)), it is seen that the solid Al truncated-tetrahedrons are much like dispersion strengthening particles distributed in the soft Mg matrix.

Based on the above discussion, it will be easy to understand surface properties of $Mg_{17}Al_{12}$. Since the bonding of Al truncated-tetrahedrons is very strong, breaking these solid Al truncated-tetrahedrons will need more power and generate a surface with high surface energy. In other words, keeping the structure integrity of Al truncated-tetrahedron is helpful to lower surface energy of $Mg_{17}Al_{12}$. In T1−T5 terminations, only the T1 termination is able to keep the structure integrity of Al truncated-tetrahedron (Fig. 6(e)). Other four terminations, for example the T3 termination (Fig. 6(f)), will destroy the Al truncated-tetrahedron. Therefore, the $Mg_{17}Al_{12}$ (110) surface with T1 termination is theoretically more stable than that with T2−T5 terminations, agreeing with experimental observation that the $Mg_{17}Al_{12}$ (110) surface interacted with Mg (0001) matrix through T1 termination [11].

The explanation on stability of T1 termination is also helpful to understand some theoretical and experimental results of $Mg_{17}Al_{12}$. For example, theoretical work indicated that the $Mg_{17}Al_{12}$ (110) surface was more stable than (100) and (111) surfaces [4,5]. In experiments, the β-$Mg_{17}Al_{12}$ precipitates preferred a $(110)_\beta//(0001)_\alpha$ Burgers orientation relationship with α-Mg matrix [6,11,23]. All these results can be easily understood by the Al truncated-tetrahedron because, among all surfaces of $Mg_{17}Al_{12}$, only the (110) surface is able to keep the integrity of Al truncated-tetrahedron through T1 termination. This advantage of (110) surface is one

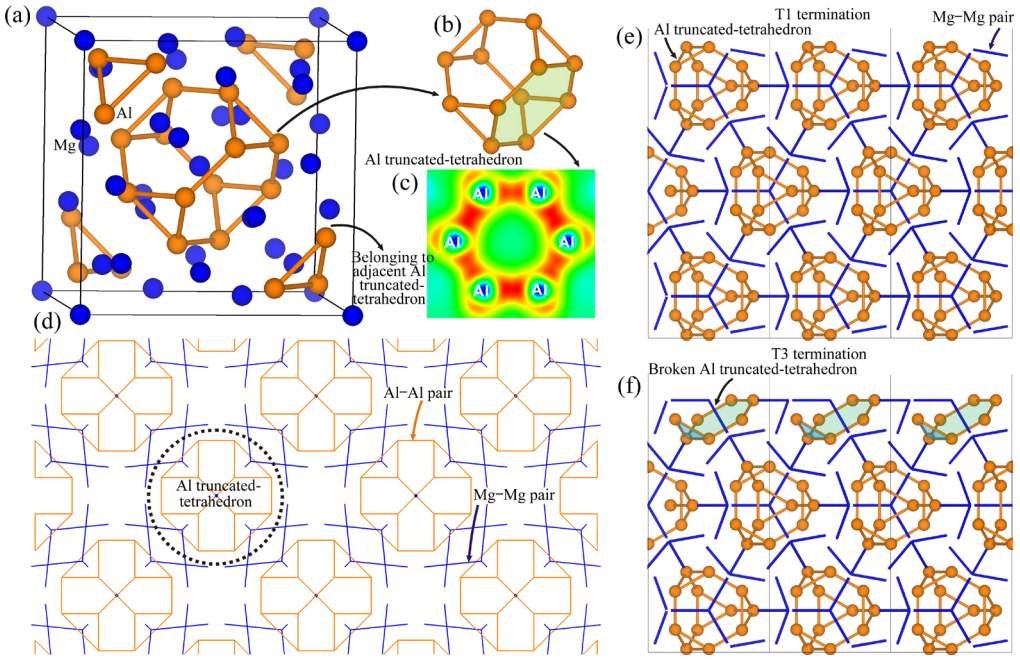

Fig. 6 Atomic structure of $Mg_{17}Al_{12}$ conventional cell (a), separate Al truncated-tetrahedrons (b), charge density (c) of shaded Al-hexagon in (b), wireframe of $Mg_{17}Al_{12}$ super-cell obeserved from [001] direction (d), and $Mg_{17}Al_{12}$ (110) surfaces with T1 (e) and T3 (f) terminations

possible reason that it is more stable than other surfaces and preferable to interacting with Mg (0001) matrix. What is worthy of mentioning is that, this advantage of (110) surface does not exclude the possibilities of $Mg_{17}Al_{12}$ exposed with other surfaces. Moreover, the possibilities of $Mg_{17}Al_{12}$ (110) surface exposed with T2−T5 terminations cannot be excluded either. Surface energy results in this study only reveal that (110) surface with T1 termination is theoretically the major part of $Mg_{17}Al_{12}$ surfaces.

3.3 Surface work function

Work function is one of the basic properties of metal surfaces [24]. For $Mg_{17}Al_{12}$, the work function property is particularly important since it is closely related to the corrosion performance of Mg−Al alloys. When β-$Mg_{17}Al_{12}$ interacts with α-Mg matrix, the work function difference at interface will induce galvanic corrosion [25−28]. Theoretically, metal with higher work function acts as cathode while that with lower work function acts as anode and corrodes first. Work function is sensitive to many factors such as adsorbates [29], surface orientations [30] and defects [31]. The above sections have investigated effects of two intrinisc defects doping on the stability of $Mg_{17}Al_{12}$ (110) surface and found that both V_{Mg} and Al_{Mg} defects are harmful to surface stabilites. However, this result does not mean that both V_{Mg} and Al_{Mg} defects are totally excluded in $Mg_{17}Al_{12}$. Actually, they are still two major intrinsic defects in $Mg_{17}Al_{12}$. Then, in this section, effects of V_{Mg} doping and Al_{Mg} doping on work function of $Mg_{17}Al_{12}$ (110) surface will be investigated.

Similar to the above sections, only the T1 and T3 terminations are simply adopted to perform work function calculations. The work function (W_f) can be obtained by the following equation [32]:

$$W_f=V-E_F \quad (3)$$

where V and E_F are vaccum energy level and Fermi level, respectivey. Using the asymmetric surface model is also able to obtain reliable work function. More calculation details of work function can be found in SI-2 in the Supporting Information. Figures 7(a) and (b) show work functions of undoped and defective $Mg_{17}Al_{12}$ (110) surfaces with T1 and T3 terminations, respectively. For visulization purpose, work functions of undoped, V_{Mg} doped and Al_{Mg} doped terminations are marked with different colors. In each figure, the horizontal solid line represents our calculated work function of Mg (0001) surface (3.68 eV), which is in good agreement with other theoretical (3.67 eV [33]) and experimental results (3.66 eV [34]). The calculation details of Mg (0001) surface can be found in SI-2 in Supporting Information. Figure 7 reveals the following two important points.

Firstly, the work function of undoped T1 termination is larger than that of Mg (0001) surface. When V_{Mg} and Al_{Mg} defects with different concentrations are doped, work functions of most defective T1 terminations (except T1+1Al_{Mg3}) are still larger than that of Mg (0001) surface. In

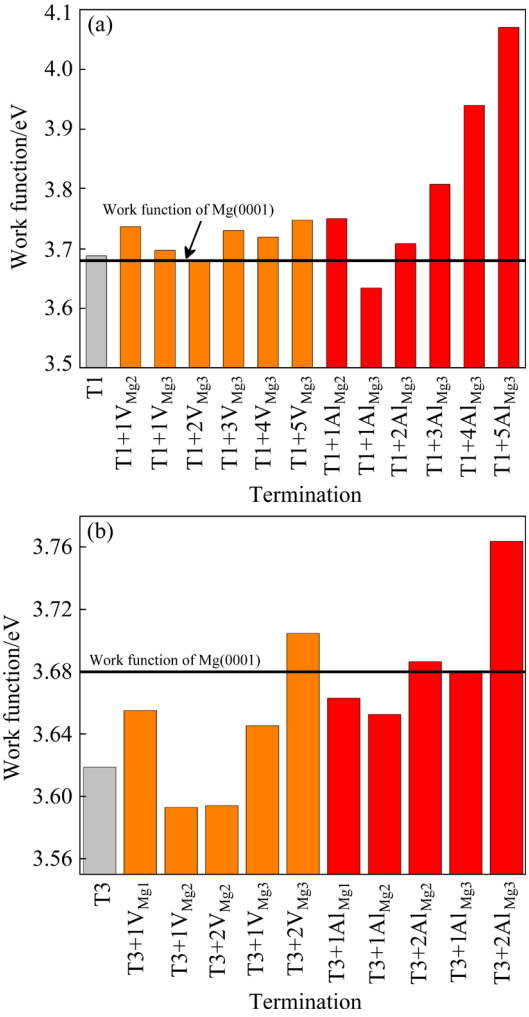

Fig. 7 Work functions of undoped and defective $Mg_{17}Al_{12}$ (110) surfaces with T1 (a) and T3 (b) terminations (Work functions of undoped, V_{Mg} doped and Al_{Mg} doped terminations are marked with different colors; The black horizontal solid line is the work function of Mg (0001) surface (3.68 eV))

contrast, work functions of undoped and most defective T3 terminations (except T3+2V_{Mg3}, T3+2Al_{Mg2} and T3+2Al_{Mg3}) are lower than that of Mg (0001) surface. This means that, in the contact between Mg and $Mg_{17}Al_{12}$, the $Mg_{17}Al_{12}$ (110) surface exposed with T1 termination is more likely to act as cathode while that with T3 termination is more likely to act as anode. $Mg_{17}Al_{12}$ and Mg in experiments act as cathode and anode, respectively, leading to the corrosion dissolution of Mg matrix [25−28]. Therefore, the work function results indirectly reveal that the $Mg_{17}Al_{12}$ (110) surface exposed with T1 termination is more consistent with practical experiments, proving the above surface energy results.

Secondly, with the increase of defect concentrations, work functions of V_{Mg} doped T1 terminations show obvious change but the change amplitude is not large compared with those of the undoped T1 termination. In contrast, work functions of Al_{Mg} doped T1 terminations show large change amplitudes. Furthermore, with the increase of Al_{Mg} concentrations, work function of T1 termination shows significant growth. Similar results can be seen in T3 termination. Work functions of Al_{Mg} doped T3 terminations also show large change amplitudes compared with those of V_{Mg} doped T3 terminations. These results indicate that the work function of $Mg_{17}Al_{12}$ (110) surface is more sensitive to the concentration change of Al_{Mg} anti-site defects. Since the above surface energy results reveal that Al_{Mg} defects are thermodynamically stabler, it is expected that the work function of $Mg_{17}Al_{12}$ (110) surface is mainly controlled by the concentration of surface Al_{Mg} defects.

It is known that galvanic corrosion is induced by work function difference of two metal surfaces. Since the work function of $Mg_{17}Al_{12}$ (110) surface is found to be mainly controlled by concentration of surface Al_{Mg} defects, it is expected that galvanic corrosion is also closely related to concentration of surface Al_{Mg} defects. Taking T1 termination as an example, when concentration of surface Al_{Mg} defects is low (for example T1+2Al_{Mg3}), the work function difference between Mg (0001) and T1 termination will be small, leading to weak corrosion of Mg anode. When concentration of surface Al_{Mg} defects increases to high content (for example T1+5Al_{Mg3}), the work function difference will be large and the galvanic corrosion will be strong. This is just one possible corrosion process of Mg−Al alloy under the variation of surface Al_{Mg} concentrations. However, this possible corrosion process may provide some insights to understand experimental results.

The addition of alloying elements such as Sc [35], Y [36] and Nd [37] is an effective method to improve the corrosion resistance of Mg−Al alloys. A common characteristic of some corrosion experiments is that, in the range of solid solubility, the corrosion resistance of Mg−Al alloys increases with the increase of the alloying elements concentrations [35−37]. For example, with the variation of Y concentration from 0 to 0.3 wt.%, the corrosion resistance of AZ91 gradually was enhanced and the best performance was achieved when the Y content was 0.3 wt.% [36]. According to our calculation results, the Y atoms may be able to substitute Mg (or Al) atoms and lower the work function of $Mg_{17}Al_{12}$ (110) surface. Then, with the variation of Y content from 0 to 0.3 wt.%, the work function difference between Mg matrix and Y added $Mg_{17}Al_{12}$ gradually decreased, leading to the improved corrosion resistance. However, this is just one possible explanation from the view of our calculation results. A detailed investigation is needed. We hope that further investigations of Mg−Al alloy, as well as other alloys, may be enlightened from this study.

4 Conclusions

(1) Whether effects of defects doping on surface stability are considered or not, the T1 termination is always the most stable termination of $Mg_{17}Al_{12}$ (110) surface. This may be ascribed to the advantage of T1 termination that, among T1−T5 terminations, only the T1 termination is able to keep the structure integrity of Al truncated-tetrahedron, while other four terminations will destroy the Al truncated-tetrahedron.

(2) The Al_{Mg} anti-site defects are more energetically favorable than Mg vacancies on the $Mg_{17}Al_{12}$ (110) surface.

(3) The $Mg_{17}Al_{12}$ (110) surface exposed with T1 termination is more likely to act as cathode in galvanic corrosion, aggreing with experiments.

(4) The work function of $Mg_{17}Al_{12}$ (110) surface is mainly controlled by the concentration of surface Al_{Mg} defects.

Acknowledgments

The authors are grateful for the financial supports from the National Natural Science Foundation of China (Nos. 11872171, 52171335, 51878246).

Supporting Information

Supporting Information in this paper can be found at: http://tnmsc.csu.edu.cn/download/08-p0755-2021-1481-supporting_information.pdf.

References

[1] KUMAR S D, KUMAR S S. Effect of heat treatment conditions on ballistic behaviour of various zones of friction stir welded magnesium alloy joints [J]. Transactions of Nonferrous Metals Society of China, 2021, 31: 156−166.

[2] LIU Fen-jun, JI Yan, BAI Yan-xia. Influence of multipass high rotating speed friction stir processing on microstructure evolution, corrosion behavior and mechanical properties of stirred zone on AZ31 alloy [J]. Transactions of Nonferrous Metals Society of China, 2020, 30: 3263−3273.

[3] ZHANG Q A, WU H Y. Hydriding behavior of $Mg_{17}Al_{12}$ compound [J]. Materials Chemistry and Physics, 2005, 94: 69−72.

[4] XIAO Wei, ZHANG Xu, GENG Wen-tong, LU Gang. Atomistic study of plastic deformation in Mg−Al alloys [J]. Materials Science and Engineering: A, 2013, 586: 245−252.

[5] WANG F X, LI B. Atomistic calculations of surface and interfacial energies of $Mg_{17}Al_{12}$–Mg system [J]. Journal of Magnesium and Alloys, 2018, 6: 375−383.

[6] NIE Jian-feng. Precipitation and hardening in magnesium alloys [J]. Metallurgical and Materials Transactions A, 2012, 43: 3891−3939.

[7] ZHANG Zi-yan, ZHOU Xing-yu, ZHANG Hong-liang, GUO Jin, NING Hua. Hydrogen penetration and diffusion on $Mg_{17}Al_{12}$(110) surface: A density functional theory investigation [J]. International Journal of Hydrogen Energy, 2017, 42: 26013−26019.

[8] ZHOU Xing-yu, MA Shu-yuan, XU Shou-lei, GUO Jin, NING Hua. Effects of Li on hydrogen absorption properties of $Mg_{17}Al_{12}$(110) surface: A density functional theory study [J]. International Journal of Hydrogen Energy, 2018, 43: 18330−18338.

[9] NING Hua, ZHOU Xing-yu, ZHANG Zi-yan, ZHOU Wen-zheng, GUO Jin. Ni catalytic effects for the enhanced hydrogenation properties of $Mg_{17}Al_{12}$(110) surface [J]. Applied Surface Science, 2019, 464: 644−650.

[10] ZHOU Xing-yu, HUANG Dan, GUO Jin, NING Hua. Hydrogenation properties of $Mg_{17}Al_{12}$ doped with alkaline-earth metal (Be, Ca, Sr and Ba) [J]. Journal of Alloys and Compounds, 2019, 774: 865−872.

[11] LIU C Q, CHEN H W, WILSON N C, NIE J F. Zn segregation in interface between $Mg_{17}Al_{12}$ precipitate and Mg matrix in Mg–Al–Zn alloys [J]. Scripta Materialia, 2019, 163: 91−95.

[12] KRESSE G, HAFNER J. Ab initio molecular dynamics for liquid metals [J]. Physical Review B, 1993, 47: 558−561.

[13] BLÖCHL C P E. Projector augmented-wave method [J]. Physical Review B, 1994, 50: 17953−17979.

[14] PERDEW J P, CHEVARY J A, VOSKO S H, JACKSON K A, PEDERSON M R, SINGH D J, FIOLHAIS C. Atoms, molecules, solids, and surfaces: Applications of the generalized gradient approximation for exchange and correlation [J]. Physical Review B, 1992, 46: 6671−6687.

[15] PERDEW J P, BURKE K, ERNZERHOF M. Generalized gradient approximation made simple [J]. Physical Review Letters, 1996, 77: 3865−3868.

[16] CRIVELLO J C, NOBUKI T, KUJI T. Limits of the Mg−Al gamma-phase range by ball-milling [J]. Intermetallics, 2007, 15: 1432−1437.

[17] SHIN D, WOLVERTON C. First-principles density functional calculations for Mg alloys: A tool to aid in alloy development [J]. Scripta Materialia, 2010, 63: 680−685.

[18] WANG Jia-jia, MA Ai-bin, LI Ming-xue, JIANG Jing-hua, CHEN Jian-qing, JIANG Ya-qing. Chemical bonding and Cu diffusion at the Cu/Ta_2N interface: A DFT study [J]. Physical Chemistry Chemical Physics, 2018, 20: 13566−13573.

[19] HU Wen-cheng, LIU Yong, HU Xiao-wu, LI De-jiang, ZENG Xiao-qin, YANG Xue, XU Ying-xuan, ZENG Xiao-shu, WANG Ke-gang, HUANG Bo-long. Predictions of mechanical and thermodynamic properties of $Mg_{17}Al_{12}$ and Mg_2Sn from first-principles calculations [J]. Philosophical Magazine, 2015, 95: 1626−1645.

[20] ZHONG Yu, YANG Mei, LIU Zi-Kui. Contribution of first-principles energetics to Al–Mg thermodynamic modeling [J]. Calphad, 2005, 29: 303−311.

[21] WANG Jin, LI Xin-xin, LIU Dan, QIN Jing-yu. The investigation on a universal local structural feature in Mg–Al alloys [J]. Computational Materials Science, 2017, 140: 224−234.

[22] SHIN D, WOLVERTON C. The effect of native point defect thermodynamics on off-stoichiometry in β-$Mg_{17}Al_{12}$ [J]. Acta Materialia, 2012, 60: 5135−5142.

[23] DULY D, ZHANG W Z, AUDIER M. High-resolution electron microscopy observations of the interface structure of continuous precipitates in a Mg−Al alloy and interpretation with the O-lattice theory [J]. Philosophical Magazine A, 1995, 71: 187−204.

[24] SKRIVER H L, ROSENGAARD N M. Surface energy and work function of elemental metals [J]. Physical Review B, 1992, 46: 7157−7168.

[25] SONG G, ATRENS A. Understanding magnesium corrosion—A framework for improved alloy performance [J]. Advanced Engineering Materials, 2003, 5: 837−858.

[26] GUSIEVA K, DAVIES C H J, SCULLY J R, BIRBILIS N. Corrosion of magnesium alloys: The role of alloying [J]. International Materials Reviews, 2015, 60: 169−194.

[27] SONG G L, ATRENS A. Corrosion mechanisms of magnesium alloys [J]. Advanced Engineering Materials, 1999, 1: 11−33.

[28] LUNDER O, LEIN J E, AUNE T K, NISANCIOGLU K. The role of $Mg_{17}Al_{12}$ phase in the corrosion of Mg alloy AZ91 [J]. Corrosion, 1989, 45: 741−748.

[29] de RENZI V, ROUSSEAU R, MARCHETTO D, BIAGI R,

SCANDOLO S, del PENNINO P U. Metal work-function changes induced by organic adsorbates: A combined experimental and theoretical study [J]. Physical Review Letters, 2005, 95: 046804.

[30] GAO Ling-yuan, SOUTO-CASARES J, CHELIKOWSKY J R, DEMKOV A A. Orientation dependence of the work function for metal nanocrystals [J]. The Journal of Chemical Physics, 2017, 147: 214301.

[31] KIM J H, HWANG J H, SUH J, TONGAY S, KWON S, HWANG C C, WU J Q, PARK J Y. Work function engineering of single layer graphene by irradiation-induced defects [J]. Applied Physics Letters, 2013, 103: 171604.

[32] SINGH-MILLER N E, MARZARI N. Surface energies, work functions, and surface relaxations of low-index metallic surfaces from first principles [J]. Physical Review B, 2009, 80: 235407.

[33] ZUO En-ci, DOU Xi-long, CHEN Ying-ying, ZHU Wen-jie, JIANG Gang, MAO Ai-jie, DU Ji-guang. Electronic work function, surface energy and electronic properties of binary Mg−Y and Mg−Al alloys: A DFT study [J]. Surface Science, 2021, 712: 121880.

[34] MICHAELSON H B. The work function of the elements and its periodicity [J]. Journal of Applied Physics, 1977, 48: 4729−4733.

[35] YAO S J, YI D Q, YANG S, CANG X H, LI W X. Effect of Sc on microstructures and corrosion properties of AZ91 [J]. Materials Science Forum, 2007, 546/547/548/549: 139−142.

[36] LUO T J, YANG Y S, LI Y J, DONG X G. Influence of rare earth Y on the corrosion behavior of as-cast AZ91 alloy [J]. Electrochimica Acta, 2009, 54: 6433−6437.

[37] YIN Zheng, HE Ren-hua, CHEN Yang, YIN Zhou, YAN Kun, WANG Kun, YAN Hong, SONG Hong-gun, YIN Cheng-xin, GUAN Hong-yu, LUO Chao, HU Zhi, LUC C. Effects of surface micro-galvanic corrosion and corrosive film on the corrosion resistance of AZ91–*x*Nd alloys [J]. Applied Surface Science, 2021, 536: 147761.

$Mg_{17}Al_{12}$(110)表面终端稳定性的密度泛函理论研究

王家佳[1]，芦子杰[1]，张开骁[2]，应国兵[1]，李保松[1]，陈建清[1]，宋 丹[1]，江静华[1]，马爱斌[1]

1. 河海大学 力学与材料学院，南京 210089；
2. 河海大学 理学院，南京 210089

摘 要： $Mg_{17}Al_{12}$(110)面具有 T1~T5 共 5 个可能的终端结构。长期以来，T3 一直被认为是该表面最稳定的终端，然而最近的理论计算表明 T1 终端可能更加稳定。为了解决这一争议，本文作者采用密度泛函理论计算揭示 $Mg_{17}Al_{12}$(110)面最稳定的终端形式。表面能计算结果表明，不论 $Mg_{17}Al_{12}$(110)面是否存在缺陷，T1 总是该面最稳定的终端。T1 终端的高稳定性可能与 $Mg_{17}Al_{12}$ 中的 Al 截角四面体有关，因为只有沿着 T1 终端截取 $Mg_{17}Al_{12}$(110)面才不会破坏 Al 截角四面体的完整性。除了揭示最稳定的终端，还计算了 $Mg_{17}Al_{12}$(110)面的功函数，结果表明该面的功函数主要由表面的 Al_{Mg} 缺陷浓度决定。

关键词： $Mg_{17}Al_{12}$；表面终端；密度泛函理论；表面能；功函数

(Edited by Wei-ping CHEN)